Permeability estimates of self-affine fracture faults based on generalization of the bottleneck concept

L. Talon,[1] H. Auradou,[1] and A. Hansen[1,2]

Received 17 July 2009; revised 2 December 2009; accepted 17 February 2010; published 17 July 2010.

[1] We propose a method for calculating the effective permeability of two-dimensional self-affine permeability fields based on generalizing the one-dimensional concept of a bottleneck. We test the method on fracture faults where the local permeability field is given by the cube of the aperture field. The method remains accurate even when there is substantial mechanical overlap between the two fracture surfaces. The computational efficiency of the method is comparable to calculating a simple average and is more than two orders of magnitude faster than solving the Reynolds equations using a finite difference scheme.

Citation: Talon, L., H. Auradou, and A. Hansen (2010), Permeability estimates of self-affine fracture faults based on generalization of the bottleneck concept, *Water Resour. Res.*, *46*, W07601, doi:10.1029/2009WR008404.

1. Introduction

[2] In many low permeability geological formations, flow occurs primarily through fracture networks [*National Academy of Sciences Committee on Fracture Characterization and Fluid Flow*, 1996]. In order to model such systems and to predict their behavior, there is a need for reliable modeling of the hydromechanical behavior of fracture. We consider in this note the situation where the shear displacement between the fracture walls strongly affects its permeability. Because of its relevance, this situation has been considered in many recent hydromechanical studies [*Archambault et al.*, 1997; *Yeo et al.*, 1998; *Hans and Boulon*, 2003; *Auradou et al.*, 2005; *Matsuki et al.*, 2006; *Watanabe et al.*, 2008; *Nemoto et al.*, 2009]. Laboratory tests report that the shearing process results in a significant channelization of the flow and an enhancement of the permeability in the direction normal to the shear. This behavior is found to be related to the long-range spatial organization of the void space, and efforts have been undertaken to modelize such system in order to provide upscaled value for the fracture permeability. Recently *Mallikamas and Rajaram* [2005] determined analytically using perturbation analysis of the Reynolds equation to the lowest nontrivial order the fracture permeability. This model, however, does not take into account the role of contact areas and will fail if they appear. The effect of contacts may, however, be taken into account by introducing an empirical parameter [*Zimmerman and Bodvarson*, 1996] that is strongly influenced by the number and the spatial distribution of the contacts [*Li et al.*, 2008].

[3] We present in this note a computational method for calculating the permeability of such fracture faults even in the presence of contacts. This new method scales linearly with the number of grid points and is more than two orders of magnitude faster than solving the finite differenced Reynolds equations through LU decomposition.

[4] There is now ample experimental and observational evidence that fracture surfaces are self affine [see, e.g., *Mandelbrot et al.*, 1984; *Brown and Scholz*, 1985; *Power et al.*, 1987; *Bouchaud et al.*, 1990; *Måly et al.*, 1992; *Schmittbuhl et al.*, 1993; *Plouraboue et al.*, 1995]. A self-affine fracture may characterized by a rescaling r of distances in the average fracture plane and a rescaling r^{ζ} of distances in the orthogonal direction leaves the statistical properties of the surface unchanged. Here ζ is the Hurst exponent. We use in the following $\zeta = 0.8$, i.e., the value often reported for rocks fractures [*Poon et al.*, 1992; *Schmittbuhl et al.*, 1993; *Matsuki et al.*, 2006]. When the two matching fracture surfaces are displaced by a distance λ along the average fracture plane, the ensuing aperture field will be self-affine up to the length scales of the order of λ. On larger scales, the aperture field settles to a constant value proportional to the average fracture opening [*Plouraboue et al.*, 1995]. This gives rise to a aperture field $h = h(x,y)$.

[5] As the two fracture surfaces approach each other, they will eventually come into contact and hence overlap. Overlap also occurs if the gap between the two fracture surfaces remains fixed while the lateral displacement λ increases. At such places of contact, we set the aperture $h(x,y)$ to zero. The contact areas are shown as white in Figure 1. The lateral displacement results in a strong structural anisotropy: The contact zones are more elongated in the direction normal to the displacement (x direction with reference to Figure 1) than in the other direction (y direction with reference to Figure 1).

[6] The idea behind the method we introduce in this note is based on the generalization of the concept of the bottleneck to higher dimensions. Some forty years ago, *Ambegaokar et al.* [1971] presented a different generalization of the same concept. As we shall see, only in a limiting case do the two generalizations approach each other.

2. Model Description

[7] Before delving into the two-dimensional generalization, and hence the method we present, we discuss the one-

[1]Laboratoire FAST, UMR 7608, Université Pierre et Marie Curie-Paris 6, Université Paris-Sud, CNRS, Orsay, France.
[2]Department of Physics, Norwegian University of Science and Technology, Trondheim, Norway.

0043-1397/10/2009WR008404

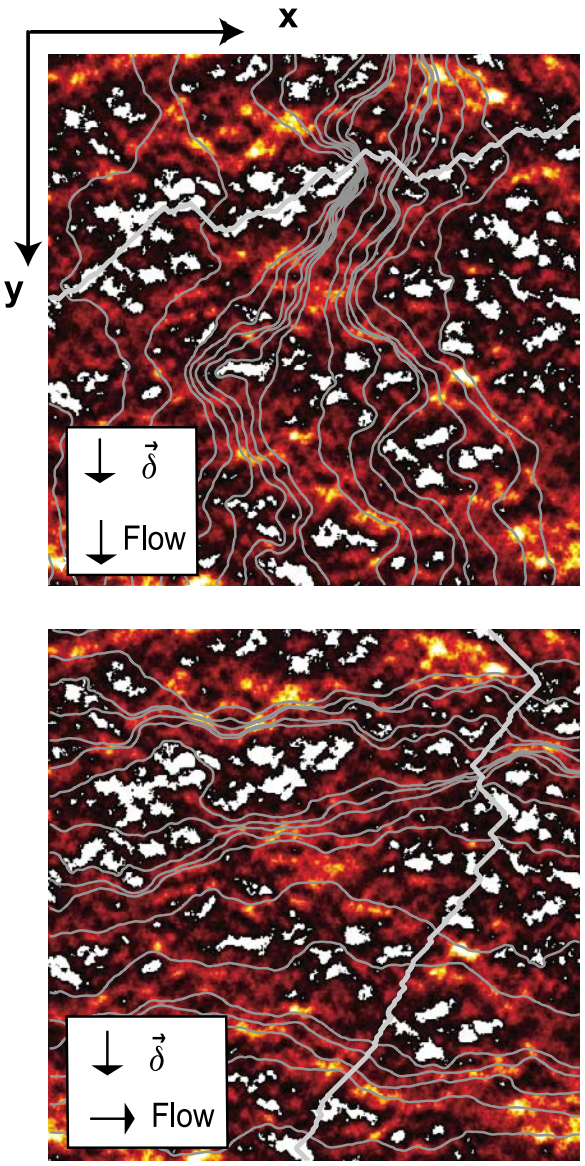

Figure 1. Aperture field obtained by shifting laterally by $\vec{\lambda} = 10\vec{e}_y$ two matching self-affine surfaces with Hurst exponent $\zeta = 0.8$. The size is 512 × 512, and the mean aperture is $\langle h \rangle = 7$. Darker shades mean smaller apertures, whereas lighter shades mean larger apertures. White zones are contact areas. The flow is (top) along and (bottom) normal to the lateral displacement $\vec{\delta}$. The flow lines are shown as grey paths. The worst paths normal to the average flow directions in the two cases are shown as thick grey lines. In Figure 1 (top), we have $\langle h^3 \rangle / \int_{\mathcal{C}} d\vec{\ell} \cdot \vec{e}_y h(\vec{\ell})^3 = 3.32$, and in Figure 1 (bottom), we have $\langle h^3 \rangle / \int_{\mathcal{C}} d\vec{\ell} \cdot \vec{e}_x h(\vec{\ell})^3 = 8.54$.

dimensional case. Hence we have a channel with self-affine walls that have been translated relative to each other along the direction of the channel by a distance λ. The channel aperture is given by $h = h(y)$, where the y axis is oriented along the channel. Assuming that the Reynolds equations govern the flow in the channel, the local permeability is proportional to $h(y)^3$. The permeability of the entire channel is then given by the harmonic mean of the local permeability, i.e., $\propto \langle h(y)^{-3} \rangle^{-1}$ [*Zimmerman and Bodvarson*, 1996]. If we now assume that the two channel walls are brought close together (so that $\langle h(y) \rangle$ decreases), the permeability is increasingly controlled by the region of minimum aperture $\min_y h(y)^3$ [*Gutfraind and Hansen*, 1995; *Skjetne et al.*, 1999], which may be then viewed as a bottleneck.

[8] How wide, Δ, is the bottleneck region? This of course depends on the geometry of the two channel walls in this region. For the time being, we leave Δ as a parameter. We now divide the entire channel along the y axis into two regions: The bottleneck region which has a width Δ and the rest which has a width $L - \Delta$, where L is the length of the entire channel. The bottleneck region have a permeability essentially given by $\min_y h(y)^3/\Delta$ and the rest of the channel will have a permeability that is essentially $\langle h^3(y) \rangle / (L - \Delta)$. The total permeability of the channel K_y may then be approximated by D_y given by

$$\frac{L}{D_y} = \frac{\Delta}{\min_y h(y)^3} + \frac{L - \Delta}{\langle h(y)^3 \rangle}. \tag{1}$$

[9] Clearly, Δ will evolve as the average channel width $\langle h(y) \rangle$ decreases and keeping it constant will constitute an approximation. How good is such an approximation? A natural choice for a fixed Δ may e.g. be the discretization length scale (i.e., the lattice constant). As $\langle h(y) \rangle$ decreases, the more dominant the bottleneck region will be and the more sensitive D_y will be to the discretization at this point. Approximations are unavoidable as the average channel width decreases. A "natural" choice as the discretization length itself breaks down when the discretization itself breaks down.

[10] We now turn to generalizing this discussion to two-dimensional aperture fields $h = h(x,y)$. The main difference between the one-dimensional channel and the two-dimensional fracture is that flow can in the latter case easily bypass regions of small aperture. They do not play the crucial role here as they did in the one-dimensional channel.

[11] We therefore generalize the concept of the bottleneck for two-dimensional fractures. As a first step to this generalization, we consider paths going from one side of the fracture to the opposite side cutting across the average flow direction. As a result of mass conservation, the flow has to pass through all such paths. For each transverse path $\mathcal{C}$ with respect to the flow direction (here, the y direction), we may calculate the average aperture cubed along it,

$$L_{\mathcal{C}} \langle h^3 \rangle_{\mathcal{C}} = \int_{\mathcal{C}} d\vec{\ell} \cdot \vec{e}_x h(\vec{\ell})^3, \tag{2}$$

where $L_{\mathcal{C}}$ is the length of the path and $\vec{e}_x$ is the unit vector in the x direction. This average now replaces for the two dimensional system, the local permeability $h^3(y)$ for the channel in one dimension.

[12] In the one-dimensional channel we then went on to identifying the smallest local permeability $\min_y h^3(y)$. This was the bottleneck. In two dimensions, we now search for the *path with the smallest average aperture cubed*, henceforth referred to as the *worst path*,

$$\min_y h(y)^3 \rightarrow \min_{\mathcal{C}} \int_{\mathcal{C}} d\vec{\ell} \cdot \vec{e}_x h(\vec{\ell})^3. \tag{3}$$

Figure 1 shows for one of the realizations the two worst paths obtained for flow directions along and normal to the lateral displacement.

[13] Using the same reasoning as in one dimension, we may now generalize equation (1) by replacing $\min_y h(y)^3$ by $\min_{\mathcal{C}} \int_{\mathcal{C}} d\vec{\ell} \cdot \vec{e}_x h t(\vec{\ell})^3$, hence

$$\frac{L}{WD_y} = \frac{\Delta}{\min_{\mathcal{C}} \int_{\mathcal{C}} d\vec{\ell} \cdot \vec{e}_x h(\vec{\ell})^3} + \frac{L-\Delta}{W\langle h(x,y)^3 \rangle}, \tag{4}$$

where W is the width of the fracture in the x direction.

[14] When the average flow is in the x direction rather than the y direction, there is of course an equivalent expression for D_x. These two expressions, for D_y and D_x, form the core of our method for approximating the permeability of fracture faults.

[15] We now discuss briefly the relation between the worst path method and the Ambegaokar-Halperin-Langer (AHL) estimate [*Ambegaokar et al.*, 1971]. The AHL estimate is based on the idea that when the local permeability is very widely distributed, the upscaled permeability is controlled by the smallest local permeability along the path connecting the inlet to the outlet that has the highest average permeability along it. If in equation (2) we assume that $h^3(x,y)$ is so widely distributed that the integral is dominated by the *largest value* of $h^3(x,y)$ along the path, the integral becomes

$$\langle h^3 \rangle_{\mathcal{C}} = \max_{\vec{\ell} \in \mathcal{C}} h(\vec{\ell})^3. \tag{5}$$

If we now combine this expression with equation (3) to estimate the permeability of the bottleneck region, we find

$$\min_{\mathcal{C}} \left[\max_{\vec{\ell} \in \mathcal{C}} h(\vec{\ell})^3 \right]. \tag{6}$$

This expression is essentially the Ambegaokar-Halperin-Langer expression for the permeability, except that we in this limit end up with the maximum permeability along the path with the minimum permeability along it, whereas in the analysis of *Ambegaokar et al.* [1971], "min" and "max" have been substituted. In two-dimensional systems, this is equivalent. Hence, only in the limit of extremely broad aperture distributions, is our formulation equivalent to that of *Ambegaokar et al.* [1971].

[16] As in one dimension, the width of the bottleneck region, Δ, is a parameter depending on the local topography near the worst path. It needs to the determined independently. One way to estimate it is to equate D_y (D_x), gotten from equation (4), with the permeability gotten from another method when the fracture opening is large: the detail of the procedure is described farther in the text. As in one dimension, we expect Δ to change as the average fracture aperture, $\langle h(x,y) \rangle$ is lowered. Assuming that it is a constant (as we will do) constitutes an approximation.

[17] Given the aperture fields, we compared their permeabilities found using equation (4) with the results of two other techniques. The first one, proposed by *Gelhar and Axness* [1983], is based on a stochastic continuum theory applied to a first order perturbation expansion of the Darcy's law. We compute numerically the Fourier transform of the permeability field perturbation $\hat{K}(k_x, k_y) = FT(h^3(x,y) - \langle h(x,y)^3 \rangle)$. The two component of the effective permeability are then calculated from the integrals

$$\frac{F_x}{\langle h^3 \rangle} = 1 - \iint \frac{k_x^2}{k^2} \frac{|\hat{K}|^2}{\langle h^3 \rangle^2} dk_x \, dk_y \tag{7}$$

and

$$\frac{F_y}{\langle h^3 \rangle} = 1 - \iint \frac{k_y^2}{k^2} \frac{|\hat{K}|^2}{\langle h^3 \rangle^2} dk_x \, dk_y. \tag{8}$$

Since this is only a second order expansion, these results are expected to be valid only for small permeability fluctuations, i.e., when the fracture opening $\langle h \rangle$ is large compared to the height fluctuations in the fracture [*Mallikamas and Rajaram*, 2005]. The second method consists in solving the flow field inside the permeability field by using a lattice Boltzmann method. In the this scheme, we introduce a body force to produce a Darcy-Brinkman equation as described by *Martys* [2001] and *Talon et al.* [2003]. We decrease the Brinkman term so that it has no appreciable effect on the permeability. When the two surfaces are in contact, the lattice site is set to be solid by using the "bounce-back" reflection method for the density distribution. A pressure-imposed boundary condition is used at the inlet and outlet as described by *Zou and He* [1997].

[18] Practically, we identify the worst path and the corresponding integral, equation (3) by using a transfer matrix algorithm [*Barabási and Stanley*, 1995]. If the average flow direction is in the y direction, the path we construct runs between the sides of the sample parallel to the x axis. We discretize the aperture field $h(x,y) \rightarrow h(i,j)$, onto a square lattice where i runs from 1 to $M = W/a$ and j from 1 to $N = L/a$, and a is the lattice constant. We introduce a second field $p(i,j)$ which initially is set to zero everywhere. We then update layer by layer in the i direction

$$p(i+1,j) = \min[p(i,j-1), p(i,j), p(i,j+1)] + h(i+1,j)^3 \tag{9}$$

until $i = M-1$. The integral equation (3) is then given by

$$p(M, j_M) = \min_j p(M,j), \tag{10}$$

where we designate by j_M the j value where the minimum p was identified. In order to reconstruct the worst path, we start at the position (M, j_M). We then move on the next layer, and identify min[$p(M-1, j_M-1)$, $p(M-1, j_M)$, $p(M-1, j_M+1)$]. The j value that corresponds to the minimum at level $i = M-1$ is designated j_{M-1}. We then repeat this algorithm until we have identified j_1. The sequence j_i where $i = 1, \cdots, M$ gives the coordinates of the worst path.

[19] In equation (8) we are assuming that the paths only connect nearest-neighbor and next-nearest-neighbor nodes on the lattice, i.e., $(i, j \pm k)$ with $(i+1, j)$ where $k = 0,1$. This may be generalized to $k = 0, \cdots, m$. In our numerical calculations presented in Figures 2 and 3 we have used $m = 2$. However, we see no appreciable difference between this value and $m = 1$.

[20] The algorithm described in equation (8) assumes that the paths do not turn back, i.e., $j_c = j_c(i)$. In very strongly

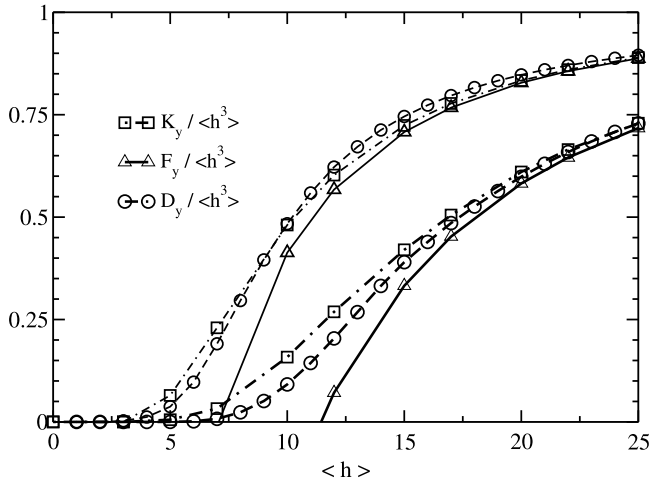

Figure 2. Normalized permeabilities of a rough fracture for flow along the lateral displacement as function of the fracture opening $\langle h \rangle$ for two lateral displacements (thick curves, $\vec{\lambda} = 10\vec{e_y}$; thin curves, $\vec{\lambda} = 20\vec{e_y}$). Circles, permeability, D_y, calculated using equation (4). Squares and triangles are for the permeabilities obtained by the lattice Boltzmann (K_y) algorithm and by the second-order perturbation theory (F_y). The system size is 512 × 512, and Δ has been set equal to 33 for $\lambda = 10$ and 38 for $\lambda = 20$ by matching D_y and F_y for the maximum fracture opening.

disordered fractures, such turns may play a role. This is not the case for the fractures studied here. However, when turns do appear, different and more involved algorithms must be used [*Hansen and Hinrichsen*, 1992; *Hansen and Kertész*, 2004]. Whereas the algorithm described in equation (8) scales as the number of nodes $M \times N$ in the discretized height field, the algorithms capable of handling overhangs scales as $M^2 \times N^2$.

3. Results

[21] We first study the situation where flow is parallel to the lateral displacement, i.e., orthogonal to the channelization. Such flow situation is illustrated in Figure 1 (top). Figure 2 shows the variation of the permeability of the fracture estimated by the lattice Boltzmann method (squares) and by the second order expansion (triangles) as functions of the mean fracture opening and for two lateral displacements. For each of the aperture fields, $p(M,j_M)$ as well as $\langle h^3 \rangle$ were measured. The estimation of D_y still requires an estimation of Δ, see equation (4). For the two lateral displacements and for large fracture openings, the second order estimate of the permeability, F_y, equation (8) fits the lattice Boltzmann K_y well. In this region, we equate F_y and D_y, hence determining Δ. We then go on to using *the same* Δ for all subsequent fracture openings. Herein lies the major approximation in our method. As soon as contact areas appear (here a noticeable difference occurs when contacts cover about 10% of the total fracture area), the perturbative estimate F_y fails to describe the continuous drop of the permeability whereas D_y remains very close to K_y.

[22] For flow normal to the lateral displacement and, as illustrated in Figure 1 (bottom), we find strong channelization and it is markedly different from the one observed when flow is parallel to $\vec{\lambda}$. Figure 3 shows the permeabilities found by the three methods: a drop off of the permeability with the fracture closure is observed but is less marked than for flow along the shift (see Figure 2 for comparison). As previously mentioned, as soon as contacts between the two surfaces occur the perturbative method fails to describe the marked permeability decrease observed with the lattice Boltzmann method. Yet the worst path method still accurately captures the permeability reduction estimate in the direction parallel to the channelization even for large lateral displacement of the fracture walls.

[23] We show in Figure 4 the relative errors between the worst path method and the lattice Boltzmann method, and the perturbative approximation and the lattice Boltzmann method for different average fracture openings. The data have been averaged over ten samples. As we see, the worst path method performs very well for all values of the average fracture opening and for the two flow directions.

4. Conclusion

[24] To conclude, we have introduced a new technique to estimate the permeability of self-affine fracture faults. Compared to other approximative methods, it performs very well by being able to reproduce the permeability closely even when the fracture opening tends to zero. "Exact" methods such as the lattice Boltzmann method gives more precise results. However, the computation time is reduced by several orders of magnitude compared to alternative methods. To our knowledge, solving the finite differenced Reynolds equations through LU decomposition is the fastest "exact method". For the samples studied in this note, the worst path method used 0.01 s per sample and per average fracture opening, whereas the LU decomposition used from 3 to 8 s. Both methods scale linearly with the number of nodes.

[25] A length scale Δ is introduced in order to fit the permeability measured. This length characterizes the extension

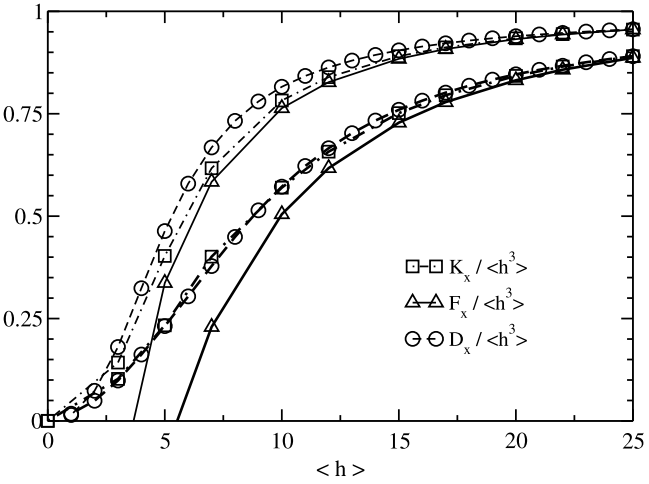

Figure 3. Normalized permeabilities of a rough fracture for flow normal to $\vec{\lambda}$ as function of the fracture opening $\langle h \rangle$ for two lateral displacements (thick lines, $\vec{\lambda} = 10\vec{e_y}$; thin lines, $\vec{\lambda} = 20\vec{e_y}$). Despite the flow direction, the conditions are similar to the ones of Figure 2, and circles, squares, and triangles refer to D_x, K_x, and F_x, respectively.

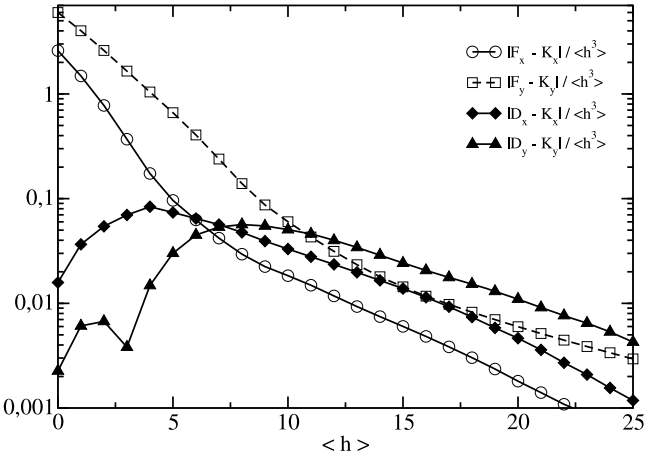

Figure 4. The relative errors $|F_x - K_x|/\langle h^3 \rangle$, $|F_y - K_y|/\langle h^3 \rangle$, $|D_x - K_x|/\langle h^3 \rangle$, and $|D_y - K_y|/\langle h^3 \rangle$ as a function of the average fracture aperture $\langle h \rangle$. The data has been averaged over 10 samples, each of size 512 × 512, Hurst exponent H = 0.8, and lateral displacement u = 10.

in the flow direction of the region dominated by the worst path. We assume that Δ remains constant as the average fracture opening is changed. This is one of the major approximation build into the method, but it allows us to determine Δ by comparison with other approximate methods such as the perturbative scheme for large enough average fracture openings for them to be accurate.

[26] Future work will be devoted to the study the relationship of between Δ and the statistics of the aperture fields.

[27] The worst path method is accurate even if the aperture field shows structural anisotropy. Such situation is achieved by laterally displacing the fracture walls leading, as observed on natural fractures, to an anisotropic permeability field. The proposed method can be further extended to other transport properties such as diffusion or electrical conductivity. Different statistical fields such as log normal permeability fields which also give rise to heterogenous flow structures will also be of interest as well as three-dimensional permeability fields.

[28] **Acknowledgments.** We thank J. P. Hulin for important comments and discussion. A.H. thanks Laboratoire FAST for hospitality during his stay at Orsay and the Université de Paris 11 for funding. This work has been greatly facilitated by the GdR 2990 HTHS and the Triangle de la Physique.

References

Ambegaokar, V., B. I. Halperin, and J. S. Langer (1971), Hopping conductivity in disordered systems, *Phys. Rev. B*, *4*, 2612–2620.

Archambault, G., S. Gentier, J. Riss, and R. Flamand (1997), The evolution of void spaces (permeability) in relation with rock joint shear behavior, *Int. J. Rock Mech. Min. Sci.*, *34*(3–4), 1–15.

Auradou, H., G. Drazer, J. P. Hulin, and J. Koplik (2005), Permeability anisotropy induced by the shear displacement of rough fracture walls, *Water Resour. Res.*, *41*, W09423, doi:10.1029/2005WR003938.

Barabási, A. L., and H. E. Stanley (1995), *Fractal Concepts in Surface Growth*, Cambridge Univ. Press, Cambridge, U. K.

Bouchaud, E., G. Lapasset, and J. Planès (1990), Fractal dimension of fracture surfaces: A universal value?, *Europhys. Lett.*, *13*, 73–79.

Brown, S. R., and C. H. Scholz (1985), Broad bandwidth study of the topography of natural rock surfaces, *J. Geophys. Res.*, *90*, 12,575–12,582.

Gelhar, L. W., and C. L. Axness (1983), Three-dimensional stochastic analysis of macrodispersion in aquifers, *Water Resour. Res.*, *19*, 161–180.

Gutfraind, R., and A. Hansen (1995), Study of fracture permeability using lattice gas automata, *Transp. Porous Media*, *18*, 131–149.

Hans, J., and M. Boulon (2003), A new device for investigating the hydro-mechanical properties of rock joints, *Int. J. Numer. Anal. Methods Geomech.*, *27*(6), 513–548.

Hansen, A., and E. L. Hinrichsen (1992), Some remarks on percolation, *Phys. Scr. T*, *44*, 55–61.

Hansen, A., and J. Kertész (2004), Phase diagram of optimal paths, *Phys. Rev. Lett.*, *93*, 040601, doi:10.1103/PhysRevLett.93.040601.

Li, B., Y. J. Jiang, T. Koyama, L. R. Jing, and Y. Tanabashi (2008), Experimental study of the hydro-mechanical behavior of rock joints using a parallel-plate model containing contact areas and artificial fractures, *Int. J. Rock Mech. Min. Sci.*, *45*(3), 362–375.

Mallikamas, W., and H. Rajaram (2005), On the anisotropy of the aperture correlation and effective transmissivity in fractures generated by sliding between identical self-affine surfaces, *Geophys. Res. Lett.*, *32*, L11401, doi:10.1029/2005GL022859.

Måly, K. J., A. Hansen, E. L. Hinrichsen, and S. Roux (1992), Experimental measurements of the roughness of brittle cracks, *Phys. Rev. Lett.*, *68*, 213–217.

Mandelbrot, B. B., D. E. Passoja, and A. J. Paullay (1984), Fractal character of fracture surfaces of metals, *Nature*, *308*, 721–722.

Martys, N. S. (2001), Improved approximation of the Brinkman equation using a lattice Boltzmann method, *Phys. Fluids*, *13*, 1807–1810.

Matsuki, K., Y. Chida, K. Sakaguchi, and P. W. J. Glover (2006), Size effect on aperture and permeability of a fracture as estimated in large synthetic fractures, *Int. J. Rock Mech. Min. Sci.*, *43*(5), 726–755.

National Academy of Sciences Committee on Fracture Characterization and Fluid Flow (1996), *Rock Fractures and Fluid Flow: Contemporary Understanding and Applications*, Natl. Acad. Press, Washington, D. C.

Nemoto, K., N. Watanabe, N. Hirano, and N. Tsuchiya (2009), Direct measurement of contact area and stress dependence of anisotropic flow through rock fracture with heterogeneous aperture distribution, *Earth Planet. Sci. Lett.*, *281*, 81–87.

Plouraboue, F., P. Kurowski, J.-P. Hulin, S. Roux, and J. Schmittbuhl (1995), Aperture of rough cracks, *Phys. Rev. E*, *51*, 1675–1685.

Poon, C. Y., R. S. Sayles, and T. A. Jones (1992), Surface measurement and fractal characterization of naturally fractured rocks, *J. Phys. D Appl. Phys.*, *25*, 1269–1275.

Power, W. L., T. E. Tullis, S. R. Brown, G. N. Boitnott, and C. H. Scholz (1987), Roughness of natural fault surfaces, *Geophys. Res. Lett.*, *14*, 29–32.

Schmittbuhl, J., S. Gentier, and S. Roux (1993), Field measurements of the roughness of fault surfaces, *Geophys. Res. Lett.*, *20*, 639–641.

Skjetne, E., A. Hansen, and J. S. Gudmundsson (1999), High-velocity flow in a self-affine channel, *J. Fluid. Mech.*, *383*, 1–28.

Talon, L., J. Martin, N. Rakotomalala, D. Salin, and Y. C. Yortsos (2003), Lattice BGK simulations of macrodispersion in heterogeneous porous media, *Water Resour. Res.*, *39*(5), 1135, doi:10.1029/2002WR001392.

Watanabe, N., N. Hirano, and N. Tsuchiya (2008), Determination of aperture structure and fluid flow in a rock fracture by high-resolution numerical modeling on the basis of a flow-through experiment under confining pressure, *Water Resour. Res.*, *44*, W06412, doi:10.1029/2006WR005411.

Yeo, I. W., M. H. De Freitas, and R. W. Zimmerman (1998), Effect of shear displacement on the aperture and permeability of a rock fracture, *Int. J. Rock Mech. Min. Sci.*, *35*(8), 1051–1070.

Zimmerman, R. W., and G. S. Bodvarson (1996), Hydraulic conductivity of rock fractures, *Transp. Porous Media*, *23*, 1–30.

Zou, Q., and X. He (1997), On pressure and velocity boundary conditions for the lattice Boltzmann BGK model, *Phys. Fluids*, *9*, 1591–1598.

H. Auradou and L. Talon, Laboratoire FAST, UMR 7608, Université Paris Sud, CNRS, Bâtiment 502, F-91405 Orsay CEDEX, France. (auradou@fast.u-psud.fr; talon@fast.u-psud.fr)

A. Hansen, Department of Physics, Norwegian University of Science and Technology, N-7491 Trondheim, Norway. (alex.hansen@ntnu.no)